Received: 19 January 2022 | Revised: 6 July 2022 | Accepted: 17 July 2022

DOI: 10.1111/gcb.16349

Global Change Biology WILEY

RESEARCH ARTICLE

Multi-season climate projections forecast declines in migratory monarch butterflies

Erin R. Zylstra[1] | Naresh Neupane[2] | Elise F. Zipkin[1]

[1]Department of Integrative Biology, Ecology, Evolution, and Behavior Program, Michigan State University, East Lansing, Michigan, USA

[2]Department of Biology, Georgetown University, Washington, District of Columbia, USA

Correspondence
Erin R. Zylstra, Tucson Audubon Society, Tucson, AZ 85705, USA.
Email: erinzylstra@gmail.com

Present address
Erin R. Zylstra, Tucson Audubon Society, Tucson, Arizona, USA

Funding information
National Science Foundation, Grant/Award Number: DBI-1954406 and EF-1702635; U.S. Geological Survey Midwest Climate Adaptation Science Center, Grant/Award Number: G21AC10369-00

Abstract

Climate change poses a unique threat to migratory species as it has the potential to alter environmental conditions at multiple points along a species' migratory route. The eastern migratory population of monarch butterflies (*Danaus plexippus*) has declined markedly over the last few decades, in part due to variation in breeding-season climate. Here, we combined a retrospective, annual-cycle model for the eastern monarch population with climate projections within the spring breeding grounds in eastern Texas and across the summer breeding grounds in the midwestern U.S. and southern Ontario, Canada to evaluate how monarchs are likely to respond to climate change over the next century. Our results reveal that projected changes in breeding-season climate are likely to lead to decreases in monarch abundance, with high potential for overwintering population size to fall below the historical minimum three or more times in the next two decades. Climatic changes across the expansive summer breeding grounds will also cause shifts in the distribution of monarchs, with higher projected abundances in areas that become wetter but not appreciably hotter (e.g., northern Ohio) and declines in abundance where summer temperatures are projected to increase well above those observed in the recent past (e.g., northern Minnesota). Although climate uncertainties dominate long-term population forecasts, our analyses suggest that we can improve precision of near-term forecasts by collecting targeted data to better understand relationships between breeding-season climate variables and local monarch abundance. Overall, our results highlight the importance of accounting for the impacts of climate changes throughout the full-annual cycle of migratory species.

KEYWORDS
climate projections, *Danaus plexippus*, full-annual-cycle model, growing degree day, monarch butterfly, population forecasts

1 | INTRODUCTION

Rapid changes in the Earth's climate disrupt wildlife population dynamics in myriad ways, by shifting or contracting species' ranges (Chen et al., 2011; Parmesan, 2006), altering demographic rates (Jenouvrier et al., 2012, 2021; Pomara et al., 2014), and inducing consequential behavioral changes (Huey et al., 2012; Rabaiotti & Woodroffe, 2019). Migratory species are particularly vulnerable to changes in climate, not just due to phenological mismatches (Both et al., 2006; Culbertson et al., 2022; Post & Forchhammer, 2008; Senner et al., 2017) or alterations to migratory routes (Curley et al., 2020; Zurell et al., 2018), but also because such species are sensitive to local environmental conditions at multiple stages of their migratory cycle (Doyle et al., 2020; Layton-Matthews et al., 2020). The dynamics of migratory populations are influenced by conditions on summer breeding grounds and overwintering sites but also

stop-over locations. Recent studies have documented alarming declines in migratory species, including a 28% drop in abundance of migratory birds in North America since 1970 (Rosenberg et al., 2019) and notable declines in high-profile migratory insects (Green et al., 2021). Effective conservation efforts for migratory species will rely on accurate spatiotemporal forecasts of population dynamics in response to potential climate changes across the annual cycle and along the migratory pathway.

One of the most dramatic declines in a migratory species over the last quarter century is that of monarch butterflies (*Danaus plexippus*) in North America. The populations both west and east of the Rocky Mountains have declined by more than 80% in the last several decades (Agrawal & Inamine, 2018; Brower et al., 2012; Schultz et al., 2017), prompting their listing as a candidate species under the U.S. Endangered Species Act (US Fish and Wildlife Service, 2020). The larger eastern population completes one of the most spectacular annual migrations in the insect world, traversing thousands of kilometers over multiple generations. In late February and early March, monarchs leave overwintering grounds in central Mexico and migrate to spring breeding grounds, centered in eastern Texas, where they lay eggs and subsequently die. The next generation continues the northward migration and arrives on summer breeding grounds, in northern parts of the eastern U.S. and southeastern Canada, in May and June. There, they produce another two to three generations. Individuals in the final generation enter reproductive diapause and begin their southward migration in late August and September, eventually making their way back to the same overwintering grounds in Mexico.

Like many insects, rapid changes in climate pose a significant threat to the eastern migratory population of monarch butterflies (Crewe et al., 2019; Halsch et al., 2021; Zylstra et al., 2021). While weather conditions in all seasons have the potential to affect monarch population dynamics, conditions in the spring and summer are particularly important as they have both direct and indirect effects on rates of monarch recruitment (Ries et al., 2015). Cumulative precipitation immediately prior to and during breeding seasons affects the quantity and quality of milkweed (*Asclepias* spp.), the sole host plant and food source for larval monarchs (Couture et al., 2015; Haan & Landis, 2020; Lemoine, 2015). Breeding-season temperatures can also influence milkweed availability, but perhaps more importantly, affect rates of development and survival in larval monarchs (Zalucki, 1982). Growing degree days (GDD), or heat accumulated over time within a species-specific temperature range, is a commonly used metric to describe insect and plant phenology (Cayton et al., 2015), providing a mechanistic link between thermal conditions and rates of monarch development and survival, and ultimately, annual population size (Edwards & Crone, 2021; Saunders et al., 2018).

Since the mid-2000s, breeding-season weather has been the primary driver of dynamics in the eastern monarch population, explaining almost seven times more variation in peak summer population size than other factors (Zylstra et al., 2021). Global climate models indicate that current weather conditions on both the spring and summer breeding ranges will shift markedly over the next century (Diffenbaugh & Field, 2013; IPCC, 2014). Understanding how the distribution and abundance of monarchs are likely to change in response to potential shifts in breeding-season climate will be a critical component in effective conservation and habitat restoration activities.

To forecast monarch population responses to expected climate changes over the next century, we combined estimates from a retrospective analysis of monarch population dynamics between 2004 and 2018 with projections of climate variables under multiple emissions scenarios for three future time periods. We combined climate projections in spring across eastern Texas with county-level projections of climate on the summer breeding grounds to forecast counts of adult monarchs throughout the midwestern U.S. and southern Ontario. We used these spatially explicit forecasts to understand how the abundance and distribution of monarchs on the summer breeding grounds may shift under a range of future emissions scenarios. Because conservation organizations and governing bodies use measures of monarch population size in early winter to assess trends and declines, we used the forecasted summer counts to generate forecasts of future overwintering monarch population sizes that account for multiple sources of climate- and model-related uncertainty.

2 | MATERIALS AND METHODS

2.1 | Population model

We adapted the modeling framework developed by Zylstra et al. (2021), which integrated data on adult monarch abundance at two different points in their migratory cycle (peak summer and early winter) with seasonal covariate data to estimate the retrospective effects of breeding-season climate on the size of the eastern monarch population between 2004 and 2018. The retrospective model was composed of two submodels. The first submodel describes variation in counts of adult monarchs on the summer breeding grounds as a function of conditions experienced during the spring and summer breeding periods (March–August), and the second submodel describes variation in population size in Mexico in early winter as a function of conditions experienced by the final generation as it leaves the summer breeding grounds and arrives on the overwintering grounds (August–December). Here, we provide an overview of monarch and covariate data and outline the structure of the model used to estimate parameters necessary to forecast future population sizes.

2.1.1 | Monarch data

We integrated count data on adult monarch butterflies from surveys conducted throughout the Midwestern summer breeding grounds, which we defined to include 545 counties in eight US states (Illinois,

Indiana, Iowa, Michigan, Minnesota, Missouri, Ohio, and Wisconsin) and census districts (hereafter, counties) in Ontario, Canada between 40° and 48°N latitude. Although some individuals in the eastern migratory population breed outside of this region (e.g., in the northeastern U.S.), we limited our analysis of summer data to the Midwest because the majority of individuals that arrive on the overwintering grounds originate from this region (Flockhart et al., 2017). The data come from five butterfly monitoring programs: region-wide surveys conducted by the North American Butterfly Association (NABA) and surveys organized by butterfly monitoring networks (BMNs) in four US states (Illinois, Iowa, Michigan, and Ohio; Figure S1). NABA surveys are located throughout the Midwestern breeding range and are typically completed once per season. During each NABA survey, one or more groups of volunteers search areas within a 25-km diameter circle and count the number of butterflies observed, by species (Oberhauser et al., 2015). We summed monarch counts across groups to calculate the total number of monarchs observed during each NABA survey. Volunteers with state BMNs survey the same locations multiple times each summer, walking fixed transects and counting the number of adult butterflies observed within a predetermined distance of the observer (Oberhauser et al., 2015). Similar to NABA counts, we used the total number of adult monarchs observed during each BMN survey. We included counts from all surveys completed between 14 June and 15 August in each year from 2004 to 2018. Data were available from all butterfly monitoring programs in all years with the exception of the Iowa and Michigan BMNs, which began surveys in 2006 and 2011, respectively.

To quantify the size of the overwintering population, we used data collected by the World Wildlife Fund–Mexico and Comisión Nacional de Áreas Naturales Protegidas on monarch aggregations in and near the Monarch Butterfly Biosphere Reserve in central Mexico (Vidal & Rendón-Salinas, 2014). Because monarchs form dense aggregations (hereafter, colonies) in stands of oyamel fir and are virtually impossible to census, observers delineate the perimeter of each colony and calculate the number of hectares occupied by monarchs, using this as an index of population size (Thogmartin et al., 2017; Vidal & Rendón-Salinas, 2014). For each year between 2004 and 2018, we summed the areas occupied across all 19 colony locations in late December, shortly after monarchs arrive on the overwintering grounds, and used this as a measure of early-winter population size (a response variable in our winter submodel).

2.1.2 | Climate data

We modeled counts of adult monarchs on the summer breeding grounds as a function of temperature and precipitation on the spring breeding grounds (i.e. eastern Texas [94°W to 100°W, 26°N to 34°N]), and temperature and precipitation across the summer breeding grounds in the Midwestern US and southern Ontario, Canada (as defined above for the monarch data). Previous analyses have shown that weather conditions on the monarch's spring and summer breeding grounds have a large impact on monarch population size during peak summer (19 July–15 August) and the subsequent winter (Saunders et al., 2016; Thogmartin et al., 2017; Zipkin et al., 2012; Zylstra et al., 2021).

We used GDD, a measure of accumulated heat within a species-specific range of temperatures (11.5–33°C; Zalucki, 1982) to assess the effects of temperature on the monarch population, as has been done in previous studies of monarchs (Saunders et al., 2018; Zipkin et al., 2012) and other Lepidoptera. For spring, we accumulated GDD between 22 March and 2 May (weeks 4–9, where we designate week 1 to begin on 1 March). In each year t (t = 1, …, 15), we obtained daily minimum and maximum temperatures for gridded points across eastern Texas, computed GDD values for each location, and averaged values across locations to generate an annual GDD value ($spGDD_t$). For summer, we used two measures to assess spatiotemporal variation in GDD on the breeding grounds: $avgGDD_c$ is the 15-year average of heat accumulated throughout the summer breeding season (weeks 10–24) in county c; $diffGDD_{c,k,t}$ measures the difference between the heat accumulated from the start of week 10 (May 3) through weeks 16–24 (indexed with k = 1, …, 9) in county c in year t and the 2004–2018 average for that county and weekly period.

To assess the effects of spring precipitation on subsequent counts of monarchs on the summer breeding grounds, we obtained monthly precipitation totals for eastern Texas in February, March, and April. We summed monthly values to generate an annual measure of spring precipitation ($spPCP_t$). For each county on the summer breeding grounds, we obtained monthly precipitation totals for April, May, June, July, and August, and summed these values to obtain an annual measure of summer precipitation. We characterized spatial variation in precipitation across the summer breeding range by averaging annual precipitation totals in each county ($avgPCP_c$), and characterized temporal variation within each county by calculating the difference ($diffPCP_{c,t}$) between annual precipitation in year t and the 15-year average. All climate data, for gridded locations in Texas and centroids of each county on the summer breeding grounds, were obtained from Daymet (Thornton et al., 2018).

2.1.3 | Other covariate data

In addition to climate-related covariates, we allowed monarch population size to vary with land cover and herbicide use. Specifically, we modeled counts on the summer breeding grounds as a function of crop cover in each county ($crop_c$) and the amount of unforested land within 12.5 km or 2.5 km of each NABA or BMN survey location, respectively ($open_{i(c)}$, where i denotes survey locations within county c). We based land cover measures in US and Canadian counties on data from the 2011 National Land Cover Database and 2010 North American Land Change Monitoring System database, respectively, assuming no change in land cover over the 15-year period (Zylstra et al., 2021). We used data on herbicide use from the U.S. Geological Survey Pesticide National System and data on corn and soybean acreage from the U.S. Department of Agriculture to calculate the proportion of corn and soybean crops treated with

glyphosate in each U.S. county and year ($gly_{c,t}$; Saunders et al., 2018; Zylstra et al., 2021). We used similar data from the Ontario Ministry of Agriculture, Food and Rural Affairs to calculate the proportion of crops treated each year in Canadian counties. When there were no data on herbicide use (28/545 counties, all of which had <9% crop cover), we imputed the minimum county-level mean (0.62) for all years.

We allowed monarch population size in early winter to vary as a function of nectar availability during autumn migration. Similar to previous studies, we used a remotely sensed measure of landscape greenness (normalized difference vegetation index; NDVI) during the first half of autumn migration (15 September–15 October) averaged over the northern migratory corridor (90°W to 105°W, 30°N to 40°N) as an annual index of nectar availability ($nectar_t$; Saunders et al., 2019; Zylstra et al., 2021). We modeled population size in early winter as a function of dense forest cover at the overwintering colonies ($forest_t$). We delineated elliptical buffers around the locations of each overwintering colony (average 369 ha) and for each year t, calculated the percent land area comprised of forest with >70% canopy cover (Ramírez et al., 2003, 2007, 2015, 2019). We averaged values across colonies to generate an annual index of dense forest cover for the entire overwintering population.

2.1.4 | Model structure and parameter estimation

The population model, which quantifies the effects of climate and other covariates on seasonal monarch population sizes between 2004 and 2018, is composed of two submodels (Zylstra et al., 2021). The summer submodel describes variation in counts of adult monarchs on the summer breeding grounds between 14 June and 15 August (weeks 16–24) as a function of climate on the spring breeding grounds and climate and land use on the summer breeding grounds. The winter submodel describes variation in the area occupied by monarchs in late December as a function of population size in the last 4 weeks of the preceding summer (i.e., peak summer population size), nectar availability during autumn migration, and the amount of dense forest cover at overwintering sites. The two submodels are linked through the estimate of peak summer population size, which is a derived parameter in the summer submodel that is subsequently used as a covariate in the winter submodel. While there is a link between seasonal population sizes within a calendar year (spring to peak summer, peak summer to December), data and modeling constraints prevent a similar link from one calendar year to the next (December to the following spring). However, this non-autoregressive temporal structure is likely to be appropriate for many insect populations, including monarchs in eastern North America, given their capacity for rapid population growth, with dynamics driven largely by environmental conditions (Roy et al., 2001).

The modeling framework described here differs from that in Zylstra et al. (2021) in a few ways. First, we modeled the total area occupied in early winter rather than the area occupied within each colony, as the goal was forecasting changes in total population size rather than understanding how the distribution of monarchs among forest patches may be affected by future climate change. Second, we included a random yearly effect in the winter submodel, an element that was not feasible to include in the Zylstra et al. (2021) model, which included spatial random effects to describe variation among overwintering colonies. Third, we excluded an index of late-winter population size (shortly before monarchs left the overwintering ground) as a covariate in the summer submodel because it explained a relatively small amount of variation in summer counts (Zylstra et al., 2021) and we had no basis on which to project these values into the future. Finally, we calculated the index of peak summer population size on the log scale to avoid bias when standardizing expected counts near zero.

We modeled counts of adult monarchs at each survey location i ($i = 1, \ldots, n_c$) in county c ($c = 1, \ldots, 545$) during week k ($k = 1, \ldots, 9$) in year t ($t = 1, \ldots, 15$) with a negative binomial distribution (specified as a Poisson-gamma mixture): $y_{i(c),k,t} \sim \text{Poisson}(\theta_{i(c),k,t})$, with mean $\theta_{i(c),k,t} = \lambda_{i(c),k,t} \times \rho_{i(c),k,t}$, where $\rho_{i(c),k,t}$ is a random variable drawn from a gamma distribution. We modeled $\lambda_{i(c),k,t}$ as a function of the expected mean count on a NABA survey in county c ($\mu_{c,k,t}$), fixed effects allowing for differences in expected counts between BMN and NABA surveys (e.g., $IL_{i(c)} = 1$ if survey $i(c)$ is part of the Illinois BMN and 0 otherwise), and the percent of surrounding area that was unforested. We accounted for variation in survey effort by including survey duration (total search hours summed across groups) as an offset ($effort_{i(c),k,t}$):

$$\begin{aligned}\log(\lambda_{i(c),k,t}) = {} & \log(\mu_{c,k,t}) + \log(\text{effort}_{i(c),k,t}) \\ & + \beta_1 \times \text{IA}_{i(c)} + \beta_2 \times \text{IL}_{i(c)} + \beta_3 \times \text{MI}_{i(c)} \\ & + \beta_4 \times \text{OH}_{i(c)} + \beta_5 \times \text{open}_{i(c)} + \varepsilon_{i(c)},\end{aligned} \tag{1}$$

where $\varepsilon_{i(c)}$ is a random effect of survey location with mean 0 and variance σ^2_{survey}, which accounts for multiple surveys at the same location as well as variation beyond that explained by survey program and other factors in the model.

We modeled the expected mean count in county c ($\mu_{c,k,t}$) as a function of week ($week_k$), temperature, and precipitation in eastern Texas in spring, and temperature, precipitation, crop cover, and glyphosate use in each county in summer:

$$\begin{aligned}\log(\mu_{c,k,t}) = {} & \alpha_0 + \alpha_{1,t} \times \text{week}_k + \alpha_{2,t} \times \text{week}_k^2 \\ & + \alpha_3 \times \text{spGDD}_t + \alpha_4 \times \text{spGDD}_t^2 + \alpha_5 \times \text{spPCP}_t \\ & + \alpha_6 \times \text{spPCP}_t^2 + \alpha_7 \times \text{avgGDD}_c + \alpha_8 \times \text{diffGDD}_{c,k,t} \\ & + \alpha_9 \times \text{diffGDD}_{c,k,t}^2 + \alpha_{10} \times \text{avgGDD}_c \times \text{diffGDD}_{c,k,t} \\ & + \alpha_{11} \times \text{avgPCP}_c + \alpha_{12} \times \text{diffPCP}_{c,t} + \alpha_{13} \times \text{diffPCP}_{c,t}^2 \\ & + \alpha_{14} \times \text{avgPCP}_c \times \text{diffPCP}_{c,t} + \alpha_{15} \times \text{crop}_c + \alpha_{16} \times \text{gly}_{c,t} \\ & + \alpha_{17} \times \text{crop}_c \times \text{gly}_{c,t} + \varepsilon_c,\end{aligned} \tag{2}$$

where ε_c is a random county-level effect with mean 0 and variance σ^2_{county}, and $\alpha_{1,t}$ and $\alpha_{2,t}$ are random coefficients with means α_{wk} and α_{wk2},

and variances σ^2_{wk} and σ^2_{wk2}, respectively. We standardized all covariates by their respective means and standard deviations.

We modeled the total area occupied by monarchs across all overwintering colonies in early winter (late December) of year t with a gamma distribution: $A_t \sim \text{Gamma}(s, r_t,)$, where s and r_t represent shape and rate parameters, respectively. We modeled the mean area occupied, $\omega_t = s / r_t$, as a function of peak population size in the preceding summer (summer_t), nectar availability during autumn migration, and the extent of dense forest cover surrounding colonies in early winter:

$$\log(\omega_t) = \gamma_0 + \gamma_1 \times \text{summer}_t + \gamma_2 \times \text{nectar}_t + \gamma_3 \times \text{forest}_t + \varepsilon_t, \quad (3)$$

where ε_t is a random year effect with mean 0 and variance σ^2_{yr}. We standardized nectar and forest covariates by their respective means and standard deviations. The estimate of peak summer population size (summer_t) was derived from the summer submodel. For each year and county in the summer breeding range, we generated expected monarch counts on NABA surveys in weeks 21–24, on the log scale, based on the county-level model (Equation 2). We calculated a mean value across the 4 weeks in each county and year, and then averaged values across counties, weighted by the amount of unforested land area in each county (a_c):

$$\text{summer}_t = \frac{\sum_{c=1}^{545}\left(a_c \times \frac{\sum_{k=6}^{9} \log(\mu_{c,k,t})}{4}\right)}{\sum_{c=1}^{545} a_c}. \quad (4)$$

We standardized the resulting annual values by a fixed mean (1.14) and standard deviation (0.58) that approximated expected values based on preliminary runs of the summer submodel.

We used a Bayesian inferential framework to estimate parameters, running the model in STAN, executed from R using the rstan package (Carpenter et al., 2017; R Core Team, 2021; Stan Development Team, 2018). We specified independent, vague priors for all parameters. We ran three Markov chains for 4000 iterations, discarded the first 3000 iterations as burn-in, and saved every third sample thereafter, leaving 1000 iterations among the three chains to summarize the posterior distribution. We assessed model convergence by inspecting trace plots and checking that Gelman-Rubin $\hat{R}$ statistics were <1.1 (Gelman & Rubin, 1992). Data and code used in analyses are available on Zenodo (Zylstra et al., 2022).

2.2 | Climate projections

We used coupled atmosphere–ocean general circulation models (GCMs), under a range of emissions scenarios, to project spring and summer climate variables into three future periods: early (2023–2043), middle (2050–2070), and end (2080–2100) of the twenty-first century. We used a systematic approach to select an ensemble of GCMs from a set of candidate models, with the goal of excluding models that were not well-suited for the region of interest, while retaining a sufficient number of models to adequately characterize present and future climate conditions and uncertainty (Cavanagh et al., 2017; Harris et al., 2014; Karmalkar et al., 2019; Neupane et al., 2022). For this, we compared observed temperatures and precipitation (data from Daymet) with modeled values from 23 GCMs acquired from the sixth iteration of the Coupled Model Intercomparison Project (CMIP6; Eyring et al., 2016; Table S1) for each year in a validation period that spanned from 1980 (the first year Daymet data are available) to 2014 (the latest year hindcasts are available for GCMs from CMIP6). For the spring breeding range in eastern Texas, we compared observed and hindcasted mean daily temperatures averaged over 22 March and 2 May and mean daily precipitation averaged over 1 February and 30 April. For the summer breeding range in the midwestern US and southern Ontario, we compared mean daily temperatures averaged over 3 May and 15 August and mean daily precipitation averaged over 1 April and 31 August. Adapting rules from Neupane et al. (2022), we selected models for which each of the four hindcasted means (spring temperature and precipitation, summer temperature and precipitation) were within 2°C and 2 mm of observed values (for temperature and precipitation, respectively), and for which at least one of the four metrics was within 1°C or 1 mm. Of the 23 GCMs in the candidate set, six met these criteria: BCC, CANESM5, CNRMESM2, FGOALS-G3, INMCM5, and IPSLCM6 (Table S1).

We used each of the six GCMs to project climate variables under four sets of conditions that reflect alternative economic and land-use development scenarios (Shared Socioeconomic Pathways; SSPs) and different representative concentration pathways (RCPs) that describe trends in atmospheric greenhouse gases (Eyring et al., 2016; O'Neill et al., 2016, 2017). The first scenario, SSP1–RCP2.6 (hereafter SSP126), represents a future with sustainable and less resource-intensive development combined with lower emissions, resulting in less than 2°C warming by 2100 (O'Neill et al., 2016). SSP2-RCP4.5 (SSP245) is a middle-of-the-road scenario, where current development and economic trends continue, resulting in moderate climate changes. The third scenario, SSP3-RCP7.0 (SSP370), assumes an increase in nationalism and competition among countries, increasing disparities and limiting global cooperation to address environmental issues. Combining these socioeconomic patterns with higher emissions, SSP370 results in moderate-to-high increases in greenhouses gases and temperatures. Finally, SSP5-RCP8.5 (SSP585) can be viewed as a "worst case" scenario, with fossil-fuel development and high emissions leading to dramatic increases in global mean temperature (O'Neill et al., 2016). For simplicity, we refer to these four sets of conditions as emissions scenarios, ranging from low (SSP126) to high (SSP585).

For each GCM, emissions scenario, and year during each of the three future time periods, we projected daily minimum and maximum temperature and daily precipitation in spring for locations throughout eastern Texas and projected daily temperatures and precipitation in summer for each county on the summer breeding grounds. For spring climate projections, we translated daily minimum and maximum temperatures (22 March–2 May) to GDD values

($spGDD_t$) and summed daily precipitation amounts (1 February–30 April) to generate a measure of cumulative precipitation ($spPCP_t$). For summer climate projections, we translated daily minimum and maximum temperatures between 3 May and 15 August to GDD values associated with weeks 10–21 (3 May–25 July), 10–22 (3 May–1 August), 10–23 (3 May–8 August), and 10–24 (3 May–15 August). We used these weekly GDD values to calculate $avgGDD_c$ and $diffGDD_{c,k,t}$ for each future time period in the same way that we calculated $avgGDD_c$ and $diffGDD_{c,k,t}$ for 2004–2018. Similarly, we summed daily precipitation totals between 1 April and 31 August, and used these annual values to calculate $avgPCP_c$ and $diffPCP_{c,t}$ for each future time period.

2.3 | Forecasting monarch population size

We used an approach similar to that used to forecast population dynamics of other species (Gauthier et al., 2016; Iles & Jenouvrier, 2019; Jenouvrier et al., 2012), wherein we assumed that the monarch population would respond to future climate variables (GDD, precipitation) in the same manner that the population responded to these variables in the recent past. Although this assumption is less likely to hold as forecast lead time increases and future climate diverges from that observed in the recent past (Fitzpatrick & Hargrove, 2009; Rollinson et al., 2021), some form of strong assumptions must be made to forecast population responses to future environmental change.

We combined parameter estimates from the 2004–2018 population model with climate projections to forecast how the monarch population may respond to future climate scenarios. For a given GCM, emissions scenario, and future time period, we began by forecasting expected monarch counts (on the log scale) in each county (for a typical 1-h NABA survey) during each week of peak summer: $\log(\mu_{c,k,t})$, where $k = 6, \ldots, 9$ and $t = 1, \ldots, 21$. We then averaged these forecasts over weeks and counties to generate an annual index of peak summer population size ($summer_t$), which we used to forecast the area occupied by monarchs in early winter (A_t).

2.3.1 | Forecasting monarch counts during peak summer

For each GCM, emissions scenario, and future time period, we created a matrix of covariate values (**X**) to forecast expected counts of monarchs in each county, year, and week during peak summer (covariates included in Equation 2). **X** included combinations of projected climate variables ($spGDD_t$, $spPCP_t$, $avgGDD_c$, $diffGDD_{c,k,t}$, $avgPCP_c$, and $diffPCP_{c,t}$) and values of crop cover ($crop_c$) and glyphosate use (gly_c) that were set equal to their respective county-level means in 2004–2018. Because each set of covariate values (i.e., each row of **X**) was associated with climate projections for February through August from a single GCM and emissions scenario, we retained any potential correlations between spring and summer weather in the same year. All covariates in **X** were standardized by 2004–2018 means and standard deviations (i.e., the same values used to standardize covariate values in the 2004–2018 population model).

To account for parameter uncertainty (i.e., uncertainty about how the monarch population responds to changes in weather), we used all samples from posterior distributions of parameters in the 2004–2018 model, rather than simply using the median or mean of posterior samples. For each posterior draw ($m = 1, \ldots, 1000$), we multiplied the vector of regression parameter estimates in the county-level model of counts on the summer breeding grounds ($\boldsymbol{\alpha_m}$) by **X**. Random effects of week ($\alpha_{1,t,m}$ and $\alpha_{2,t,m}$) were drawn from normal distributions with means $\alpha_{wk,m}$ and $\alpha_{wk2,m}$ and standard deviations $\sigma_{wk,m}$ and $\sigma_{wk2,m}$, respectively. We assumed that the random effects of county on summer population size ($\varepsilon_{c,m}$) were equal to the estimated random effects in 2004–2018 (e.g., $\varepsilon_{1,m}$ [2023–2043] = $\varepsilon_{1,m}$ [2004–2018]).

2.3.2 | Forecasting the area occupied by monarchs in early winter

For each year and posterior draw, we averaged the forecasted log counts across weeks and counties to generate an annual index of peak summer population size ($summer_{t,m}$), which we standardized by the 2004–2018 mean and standard deviation. We used this standardized value, in conjunction with parameter estimates from the winter submodel ($\boldsymbol{\gamma_m}$), and random yearly effects ($\varepsilon_{t,m}$ drawn from a normal distribution with mean 0 and standard deviation $\sigma_{yr,m}$) to generate the expected area occupied in year t ($\omega_{t,m}$). We used the 2004–2018 means (i.e., standardized values of zero) for values of dense forest cover ($forest_t$) and nectar availability ($nectar_t$). Although it is possible that forest cover and nectar availability will vary from these means in the future, we had no data to inform such projections and thought such changes would be unlikely to meaningfully affect results given that forest cover and nectar availability had little influence on monarch population sizes between 2004 and 2018 (Table 1). Finally, we drew forecasted areas ($A_{t,m}$) from a gamma distribution with mean $\omega_{t,m}$ and shape parameter, s_m.

2.3.3 | Summarizing forecasts during each period

Although we combined parameter estimates and climate projections to make annual forecasts, we based inferences about future monarch populations on the mean, and associated variance, of forecasted values over each 21-year time period. This choice was dictated by the non-autoregressive structure of our population model, where monarch population size in 1 year is independent of population size the year before. Consequently, variation in annual forecasts (based on a single climate model, emissions scenario, and set of parameter estimates) is due solely to interannual variation in projected climate variables (Figure S2). Collectively, annual forecasts of counts

TABLE 1 Parameter estimates from a full-annual-cycle model describing the effects of climate and environmental factors on monarch population size, 2004–2018. We present mean and 95% credible intervals (95% CI) based on 1000 samples from the posterior distributions of parameters in the retrospective annual-cycle model of seasonal monarch population sizes. Parameters in the summer submodel describe variation in the number of monarchs observed during surveys conducted on the midwestern summer breeding grounds. Parameters in the winter submodel describe variation in the area occupied by monarchs on the Mexican overwintering grounds in late December. Notations correspond with those used in the text. PCP = precipitation

Parameter	Notation	Mean	95% CI
Summer submodel			
Intercept	α_0	1.42	1.23, 1.61
Week (linear)	week_k	0.68	0.55, 0.80
Week (quadratic)	week_k^2	−0.24	−0.38, −0.12
Spring GDD (linear)	spGDD_t	0.35	0.30, 0.39
Spring GDD (quadratic)	spGDD_t^2	−0.25	−0.31, −0.19
Spring PCP (linear)	spPCP_t	−0.23	−0.27, −0.19
Spring PCP (quadratic)	spPCP_t^2	−0.33	−0.36, −0.30
Summer GDD, average	avgGDD_c	−0.07	−0.24, 0.10
Summer GDD, difference (linear)	$\text{diffGDD}_{c,k,t}$	0.32	0.28, 0.36
Summer GDD, difference (quadratic)	$\text{diffGDD}_{c,k,t}^2$	−0.06	−0.08, −0.04
Summer GDD, average × difference	$\text{avgGDD}_c \times \text{diffGDD}_{c,k,t}$	−0.14	−0.18, −0.11
Summer PCP, average	avgPCP_c	0.02	−0.14, 0.20
Summer PCP, difference (linear)	$\text{diffPCP}_{c,t}$	0.17	0.15, 0.19
Summer PCP, difference (quadratic)	$\text{diffPCP}_{c,t}^2$	−0.02	−0.04, −0.01
Summer PCP, average × difference	$\text{avgPCP}_c \times \text{diffPCP}_{c,t}$	0.04	0.01, 0.07
Glyphosate use	$\text{gly}_{c,t}$	−0.08	−0.11, −0.05
Crop cover	crop_c	0.09	−0.04, 0.23
Glyphosate use × Crop cover	$\text{gly}_{c,t} \times \text{crop}_c$	−0.03	−0.05, 0.00
IA BMN (indicator)	IA_i	0.17	−0.23, 0.58
IL BMN (indicator)	IL_i	0.22	−0.08, 0.51
MI BMN (indicator)	MI_i	−1.13	−1.41, −0.85
OH BMN (indicator)	OH_i	−0.90	−1.20, −0.57
Unforested area	open_i	0.14	0.05, 0.22
SD, random effect of week (linear)	σ_{wk}	0.23	0.16, 0.34
SD, random effect of week (quadratic)	σ_{wk2}	0.25	0.17, 0.38
SD, random effect of county	σ_{county}	0.27	0.13, 0.42
SD, random effect of survey location	σ_{survey}	0.88	0.82, 0.94
Winter submodel			
Intercept	γ_0	1.20	0.82, 1.66
Summer population size	summer_t	0.37	−0.07, 0.81
Dense forest cover	forest_t	0.23	−0.19, 0.69
Nectar availability	nectar_t	0.04	−0.34, 0.40
SD, random effect of year	σ_{yr}	0.23	0.01, 0.66

on the summer breeding range or area occupied on the overwintering grounds for a given climate model, emissions scenario, and time period are expected to capture variation that would naturally occur over a 21-year period, even if the forecasted value for any 1 year is not particularly meaningful.

2.3.4 | Decomposing uncertainty in forecasts of early-winter population size

Our forecasts account for numerous sources of uncertainty, including that associated with climate projections (GCM, emissions scenario, and interannual variability), the monarch population model (parameter uncertainty), and unmodeled sources of temporal variation in monarch population size (environmental stochasticity). We used a sequential approach to assess the relative contributions of climate projection uncertainty, parameter uncertainty, and environmental stochasticity to the total amount of uncertainty associated with forecasted population size in early winter. Specifically, we generated forecasts that accounted for (1) only climate uncertainty, (2) only parameter uncertainty, (3) climate uncertainty and parameter uncertainty (excluding environmental stochasticity), and (4) all sources of uncertainty. To generate forecasts that did not account for parameter uncertainty (1st set of forecasts), we used the median of posterior distributions, rather than all posterior samples, for parameters in the 2004–2018 model. To generate forecasts that did not account for climate uncertainty (second set of forecasts), we used climate projections from one of the GCMs (CNRMESM2) under a moderate-to-high emissions scenario (SSP370). Finally, to generate forecasts that did not account for environmental stochasticity (1st, 2nd, and 3rd sets of forecasts), we simplified both the summer and winter submodels. In the summer submodel, we treated linear and quadratic effects of week as constant fixed effects rather than random effects that changed with year (i.e., we used posterior samples from α_{wk} and α_{wk2} rather than $\alpha_{1,t}$

and $\alpha_{2,t}$ drawn from normal distributions with means α_{wk} and α_{wk2}). In the winter submodel, we excluded the random effect of year (ϵ_t) and used the expected area occupied (ω_t) rather than a value drawn from a gamma distribution (A_t) with mean ω_t. To assess the relative contributions of climate uncertainty, parameter uncertainty, and environmental stochasticity, we compared the widths of 90% credible intervals among the four sets of forecasts.

3 | RESULTS

3.1 | Population model

Similar to results from Zylstra et al. (2021), breeding-season climate had the largest effects on monarch population size during peak summer, 2004–2018. Larger monarch populations were associated with moderate spring climate conditions in eastern Texas (GDD and precipitation near 2004–2018 means) and wetter conditions on the summer breeding grounds (Table 1). Monarch abundance was also positively associated with weekly GDD throughout most of the Midwestern summer breeding range, except in warmer counties, where abundance began to decline when GDD values were well above normal (Table 1; figure 4c in Zylstra et al., 2021). Ultimately, breeding-season climate was also an important driver of overwintering population size, as the number of hectares occupied by monarchs shortly after their arrival in Mexico was strongly and positively associated with counts of adult monarchs during peak summer (Table 1).

3.2 | Climate projections

The GCMs project that climate in eastern Texas will not change substantively in the near term (Figure 1a). However, by the middle and late twenty-first century, GDD values (accumulated heat between 22 March and 2 May) are expected to increase substantially, particularly under moderate or high emissions scenarios (Figure 1b,c). On average, precipitation in eastern Texas is expected to be similar to that experienced in the recent past, though there is likely to be more interannual variation than was observed in 2004–2018. Across the summer breeding grounds, projected changes in climate vary markedly, with some areas expected to become hotter but not wetter and other areas expected to see increases in both temperatures and precipitation (Figure S3). Temperatures in the southeastern portion of the monarch's summer breeding range are projected to increase little over the next 20 years (Figure 2a,b). In all other locations and under all other climate scenarios, however, GDD is expected to increase, with the largest increases (up to 137%) occurring at the highest latitudes (Figure 2). There was strong evidence of an east–west gradient in precipitation changes across the summer breeding range. Under all climate scenarios, eastern parts of the summer breeding range are projected to become wetter than conditions experienced in 2004–2018, whereas locations in Minnesota and Iowa are likely to receive similar amounts, or even less, rainfall than that received in the recent past (Figure 3).

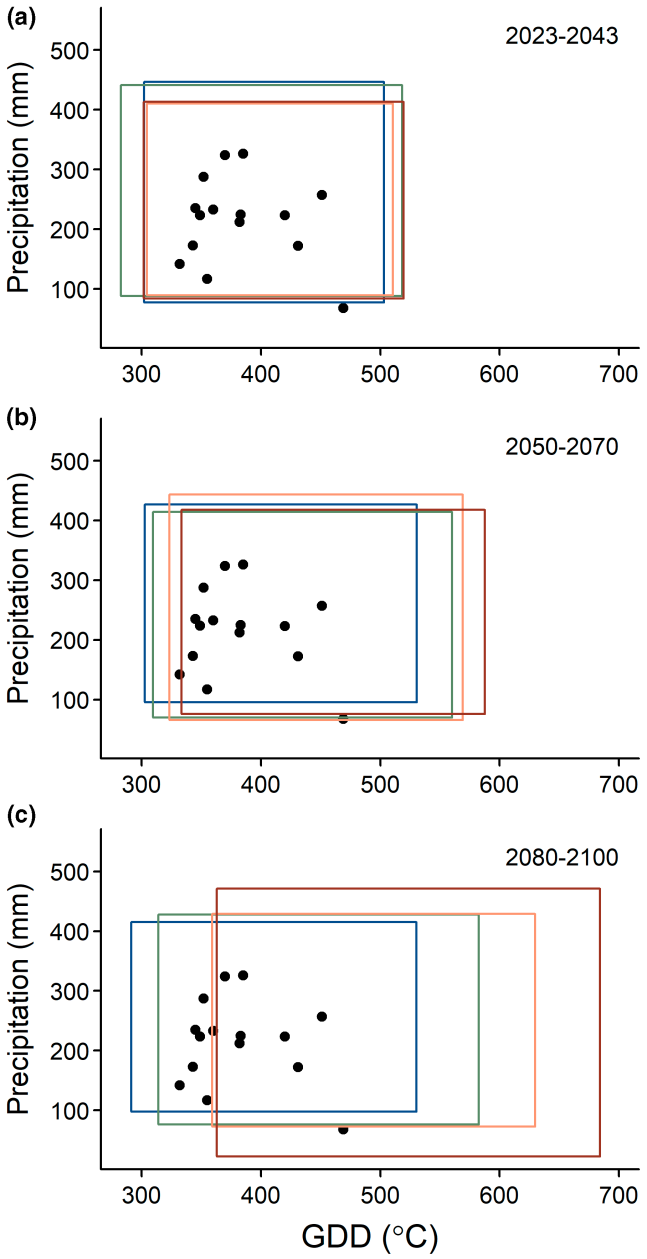

FIGURE 1 Climate projections for the monarch butterfly's spring breeding grounds. Projected temperatures (GDD = growing degree days, 22 March–2 May) and precipitation (cumulative precipitation, February–April) in eastern Texas, during three future time periods: 2023–2043 (a), 2050–2070 (b), and 2080–2100 (c). Boxes show time period means ±2 standard deviations for projections from six GCMs based on different emissions scenarios, where blue = low emissions (SSP126), green = moderate emissions (SSP245), orange = moderate-to-high emissions (SSP370), and red = high emissions (SSP585). Points show the 2004–2018 observed values. [Colour figure can be viewed at wileyonlinelibrary.com]

3.3 | Forecasted size of the monarch population in peak summer

Counts of adult monarchs during peak summer (our index of the size of the monarch population during the summer breeding season)

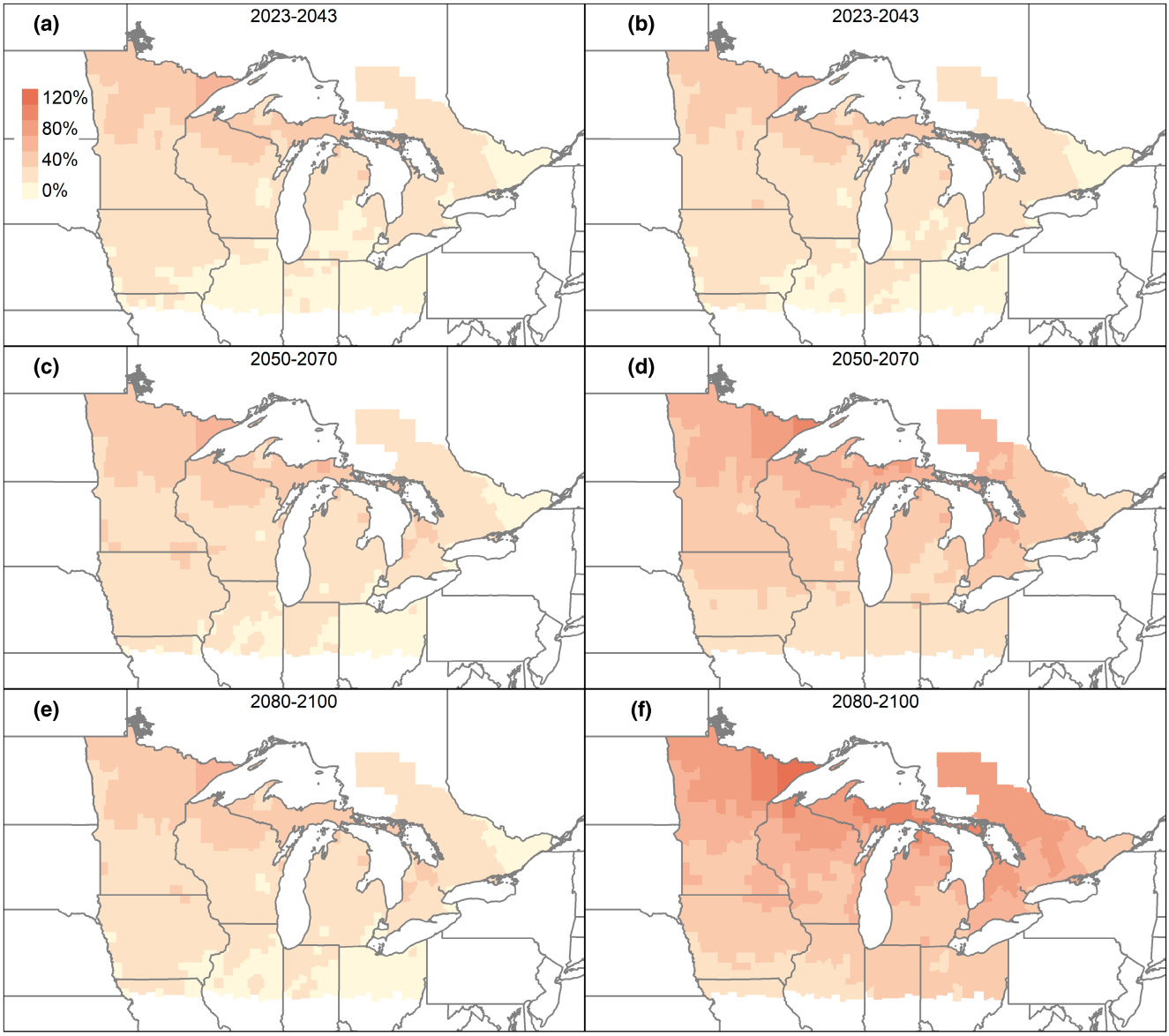

FIGURE 2 Temperature projections for the monarch butterfly's summer breeding grounds. Projected percentage change in growing degree days (GDD), 3 May–15 August, from 2004 to 2018 means averaged across six GCMs and 21 years within each of three future time periods: 2023–2043 (a, b), 2050–2070 (c, d), 2080–2100 (e, f). Panels in the left column (a, c, e) show projections under a low-emissions scenario (SSP126) and panels in the right column (b, d, f) show projections under a high-emisisons scenario (SSP585). Darker red colors indicate greater percent increases in GDD. [Colour figure can be viewed at wileyonlinelibrary.com]

are expected to decrease throughout much of the Midwestern U.S. and southern Ontario across all emissions scenarios and time periods (early [2023–2043], mid [2050–2070], and late [2080–2100] twenty-first century; Figure 4). By the end of the twenty-first century, when spring temperatures are projected to greatly exceed 2004–2018 values under all but the lowest emissions scenario (Figure 1), forecasted counts of monarchs on the summer breeding grounds are expected to be 19%–89% lower than during 2004–2018. Under a high-emissions scenario, monarchs may become scarce throughout the entire Midwestern breeding range by the end of the century, with the median forecasted count on a survey below one adult monarch per hour (2004–2018 median counts in each county ranged from 2.1 to 5.3; Figure S4). Over shorter time horizons and less severe emissions scenarios, however, the severity of forecasted declines on the Midwestern summer breeding grounds varies geographically. The steepest declines are expected in northern regions, where GDD values accumulated over the entire summer are expected to increase the most (Figure 2). Although summer precipitation has a smaller effect on the monarch population than temperatures (Table 1), monarch counts in the southern part of the summer breeding range reflect a strong east–west gradient in projected precipitation (Figures 3 and 4). In particular, monarch counts are forecasted to increase slightly over the next 20 years in areas like

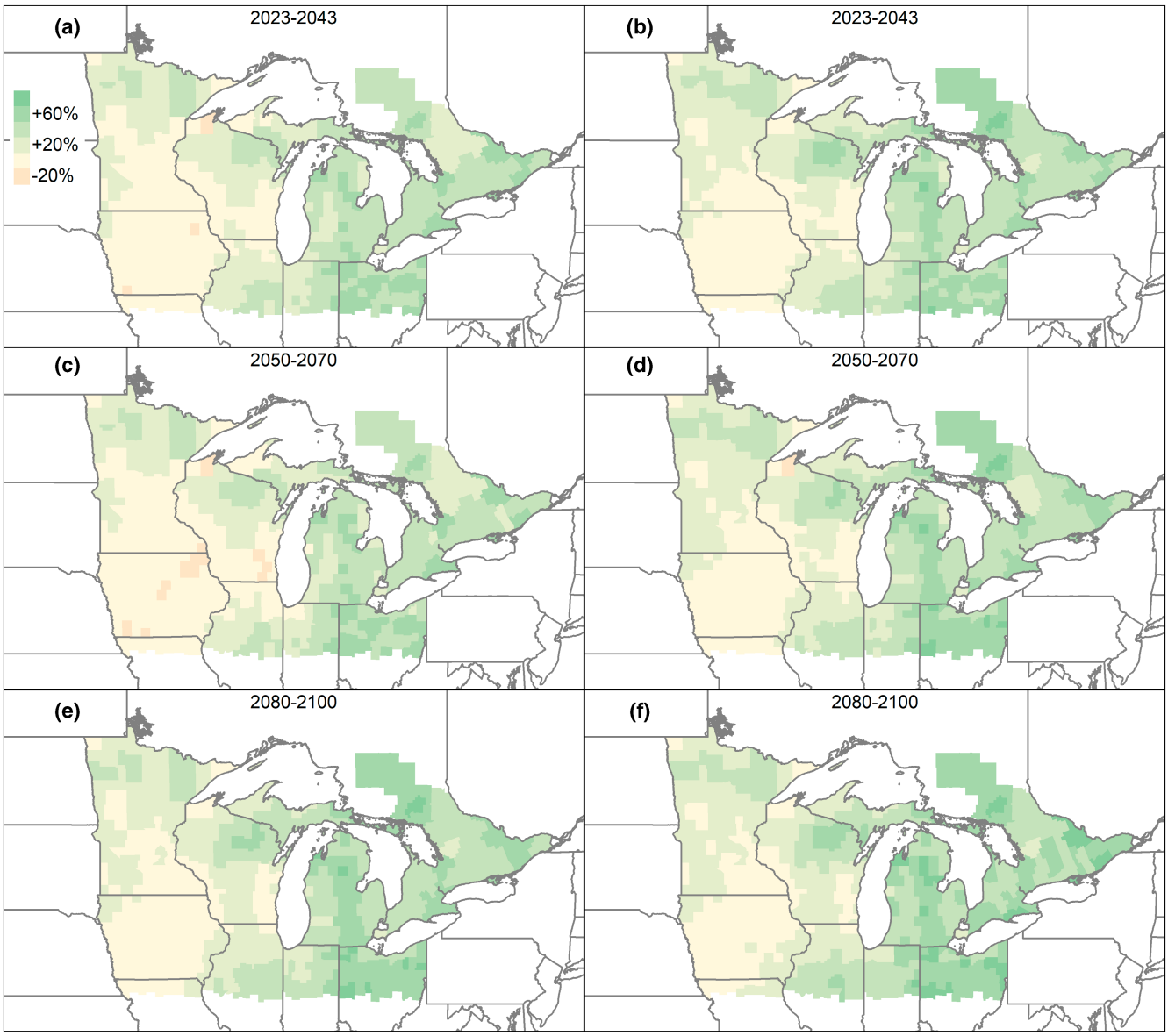

FIGURE 3 Precipitation projections for the monarch butterfly's summer breeding grounds. Projected percentage change in cumulative precipation, April–August, from 2004 to 2018 means averaged across six GCMs and 21 years within each of three future time periods: 2023–2043 (a, b), 2050–2070 (c, d), 2080–2100 (e, f). Panels in the left column (a, c, e) show projections under a low-emissions scenario (SSP126) and panels in the right column (b, d, f) show projections under a high-emisisons scenario (SSP585). Green colors indicate an increase in precipitation, brown colors indicate a decrease in precipitation, and yellow indicates little or no change. [Colour figure can be viewed at wileyonlinelibrary.com]

northern Ohio, which are projected to be wetter but not hotter (Figure 4, Figure S3).

3.4 | Forecasted size of the monarch population in early winter

Under lower emissions scenarios, forecasted monarch population size in early winter (an index summarizing the total area occupied by monarchs, in hectares) averaged over 21-year time periods is only slightly lower than the mean area occupied by monarchs during 2004–2018 (Figure 5a–c). However, under moderate-to-high emissions scenarios, the forecasted mean area occupied drops precipitously by the end of the century (orange and red values in Figure 5c) as a result of increased temperatures across the spring breeding range in eastern Texas and increased temperatures in the northern part of the Midwestern summer breeding range. Despite only modest decreases in the mean area occupied through 2070, there is a high probability that overwintering population sizes will fall below the minimum observed population size (0.67 ha in 2013) at least once during each 21-year period, even in the near term under a low emissions scenario (Figure 5d–f, Table S2). In each emissions scenario, the population is forecasted to occupy <0.67 ha for an average of three winters between 2023 and 2043 (90% credible interval: 0–8 winters) (Figure 5d).

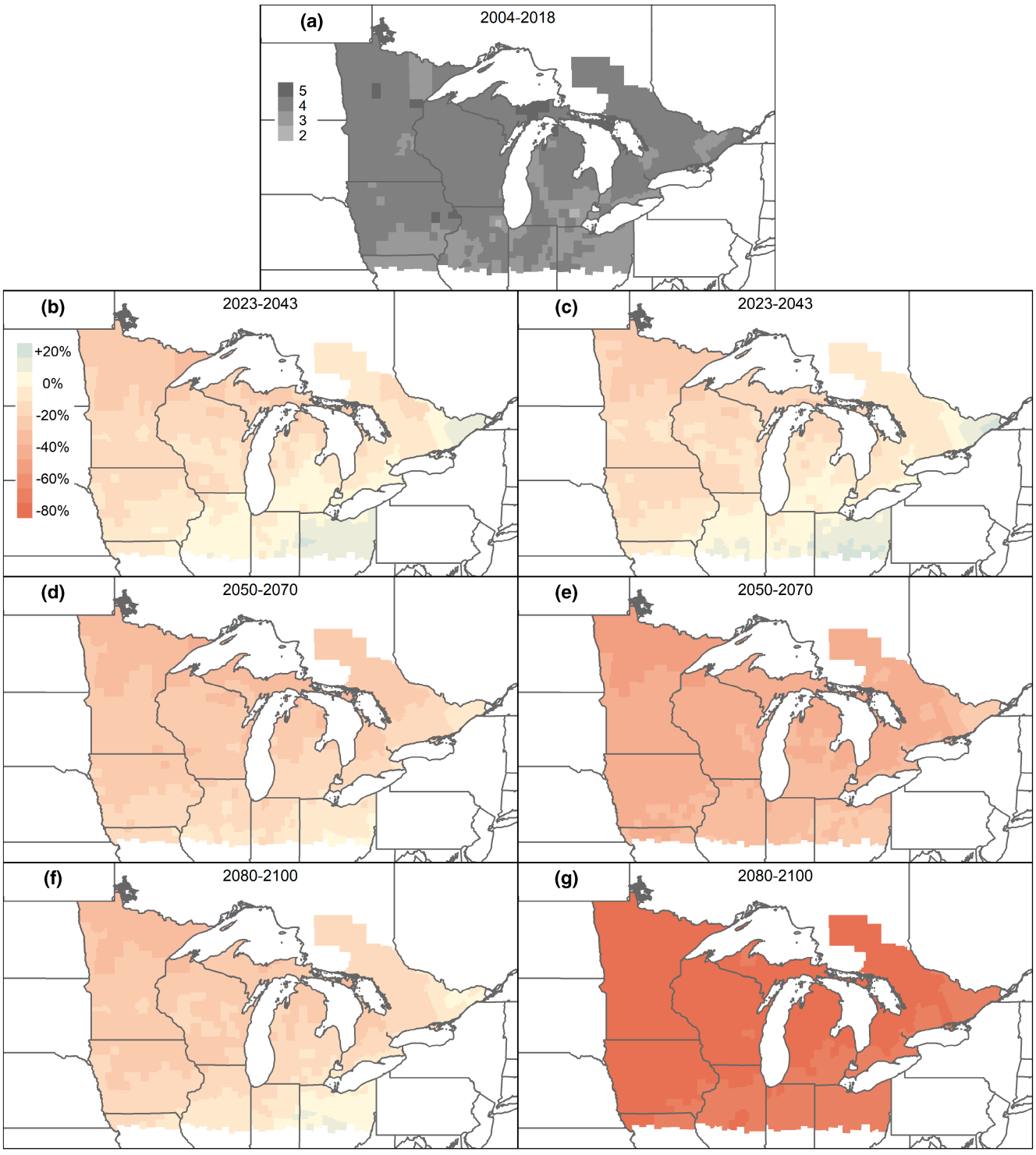

FIGURE 4 Forecasted percent change in monarch counts across the midwestern summer breeding grounds between 2004 and 2018 and each of three future time periods. Model-based estimates of 2004–2018 mean counts (number of adult monarchs observed per survey hour in an unforested area [e.g., point location with 75% open habitat] of each county during peak summer, 19 July–15 August; (a), and forecasted percentage change in counts between 2004–2018 and 2023–2043 (b, c), between 2004–2018 and 2050–2070 (d, e), and between 2004–2018 and 2080–2100 (f, g). Panels in the left column (b, d, f) depict changes under a low-emissions scenario (SSP126) and panels in the right column (c, e, g) depict changes under a high-emissions scenario (SSP585). Light blue colors indicate counties where monarch counts are expected to increase and red colors indicate counties where monarch counts are expected to decrease, while yellow colors indicate little to no change. [Colour figure can be viewed at wileyonlinelibrary.com]

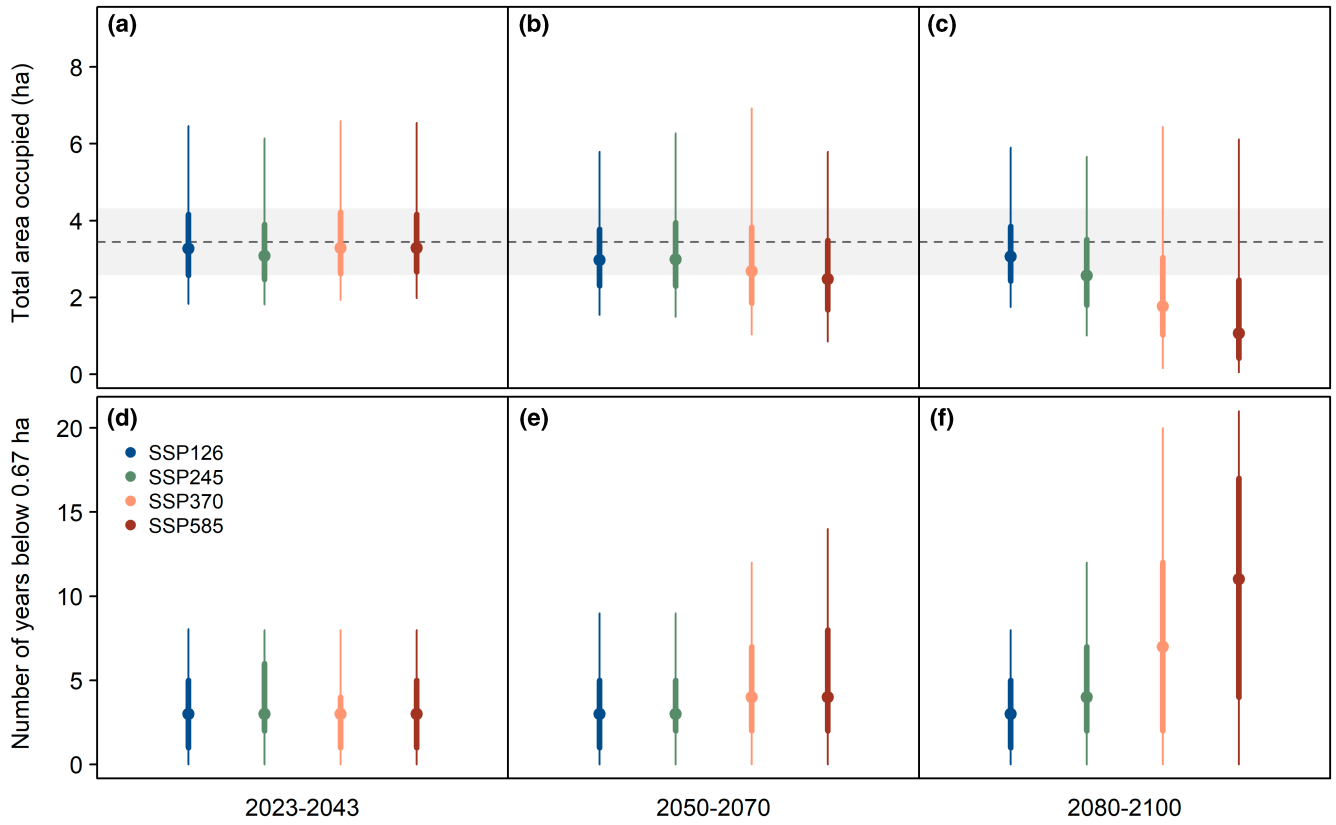

FIGURE 5 Forecasted mean area occupied by monarch butterflies on the overwintering grounds, and the number of years during each of three future time periods that the area occupied is projected to fall below the minimum size ever observed. Panels in the top row depict 21-year means of forecasted annual area occupied during early (a, 2043–2043), mid (b, 2050–2070), and late (c, 2080–2100) twenty-first century, based on four emissions scenarios, each used as input in six GCMs. The horizontal dashed line shows the mean area occupied between 2004 and 2018, and the gray shaded area represents a 90% confidence interval for the observed mean. Panels in the bottom row depict the number of years forecasted during early (d), mid (e), and late (f) twenty-first century in which the area occupied by overwintering monarchs is projected to be less than 0.67 hectares (the minimum observed). In all panels, plotted values show the medians (circles) with 50% and 90% credible intervals (thick and thin error bars, respectively) for distributions of forecasted values that account for uncertainty in GCM structure and parameter estimates, as well as environmental stochasticity. [Colour figure can be viewed at wileyonlinelibrary.com]

3.5 | Uncertainties in forecasted overwintering population size

Similar to near-term forecasts for other climate-sensitive species (Gauthier et al., 2016; Jenouvrier et al., 2020), parameter uncertainty, or uncertainty about the relationship between monarch population size and weather variables, contributes more to the total amount of uncertainty associated with forecasted population size in 2023–2043 than does climate uncertainty (54% vs 29%, respectively; Figure 6). The large amount of parameter uncertainty suggests that even if we could make precise climate projections in the near term, forecasts of the mean number of hectares occupied by overwintering monarchs are likely to remain imprecise (i.e., 90% credible interval for forecasts of the mean area occupied in 2023–2043 that only account for parameter uncertainty range from 2.03 to 4.48 ha). As forecast lead time increases, however, so does the relative contribution of climate uncertainty, primarily due to large variations in climate projections across emissions scenarios during 2080–2100 (Hawkins & Sutton, 2009). Uncertainty in population forecasts will always increase with forecast lead time, and there are limited options for reducing climate uncertainty other than selecting a subset of available GCMs for projections based on their ability to accurately model historical values of relevant climate variables within the geographic region of interest (Neupane et al., 2022). However, parameter uncertainty can be reduced, over the near and long term, by collecting targeted data to better understand mechanistic links between breeding-season temperatures and precipitation and local monarch abundance (Iles & Jenouvrier, 2019).

4 | DISCUSSION

Many species migrate to take advantage of seasonally variable resources, but these spectacular movements present risks to individuals, and potentially to populations, if anthropogenic changes in climate or land use alter the timing of resource availability or migratory behaviors (Both et al., 2006). Climate-induced changes in the environmental conditions experienced by individuals within seasonal ranges or along migratory routes pose an additional risk. Physiological and demographic responses to climate change

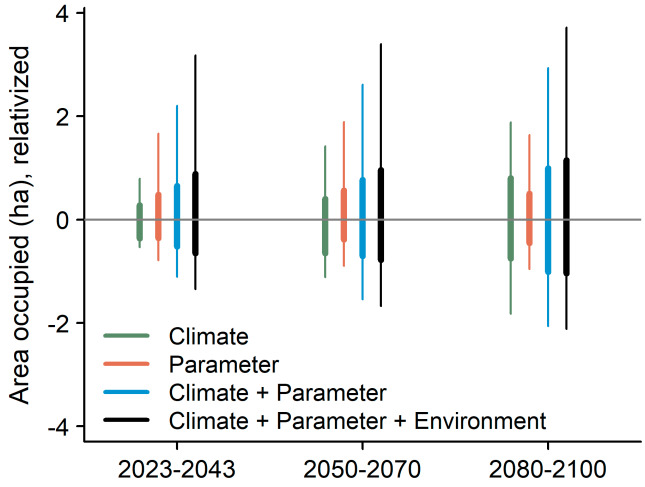

FIGURE 6 Forecasted area occupied by monarch butterflies in early winter (standardized to zero) for three future time periods, accounting for various sources of uncertainty. 21-year means of the annual forecasted area occupied, standardized to zero, during early (2043–2043), mid (2050–2070), and late (2080–2100) twenty-first century. Thick and thin vertical lines represent 50% and 90% credible intervals, respectively). Values in green, blue, and black account for climate uncertainty (six GCMs, each under four emissions scenarios), whereas values in orange are based on climate projections from a single GCM (CNRMESM2) under a moderate-to-high emissions scenario (SSP370). Values in orange, blue, and black account for parameter uncertainty (full posterior distributions of parameter estimates from the 2004 to 2018 population model), whereas the values in green use only the median parameter estimates. Values in black are the only forecasts that account for environmental stochasticity (annual variation in monarch population sizes not associated with climate and other factors in the population model). [Colour figure can be viewed at wileyonlinelibrary.com]

could have population-level consequences, particularly if climatic changes occur at multiple stops along a migratory route. Here, we show that projected changes in climate on both the spring and summer breeding grounds are likely to result in decreased abundance of monarchs in eastern North America. Long-term population declines are likely to be driven by increases in spring breeding-season temperatures, as climate in eastern Texas has had significant effects on monarch abundance in the recent past (Table 1; Crewe et al., 2019; Zylstra et al., 2021) and temperatures in this region are projected to increase dramatically in the latter half of the twenty-first century under most emissions scenarios (Figure 1). Monarch abundance on the Midwestern summer breeding grounds will vary geographically as a function of local weather conditions. Although it has proved challenging to identify mechanistic links between temperature, precipitation, and monarch population sizes, associations between climate and monarch abundances are clear (Crewe et al., 2019; Saunders et al., 2016; Zylstra et al., 2021). The size of the overwintering monarch population in a given year reflects climatic conditions experienced by monarchs over several generations. Thus, the future sizes of the overwintering population will be shaped not just by a directional change in spring temperatures, for example, but also by changes in multiple climatic variables, from local to regional scales across eastern North America.

For the last several decades, researchers have assessed the status and trends of the eastern migratory population of monarch butterflies by evaluating changes in the size of the population in early winter at their colony locations in central Mexico. Population assessments are based on this stage of the migratory cycle because the vast majority of individuals in the population are located in a small geographic region (versus other seasons, when individuals disperse over much larger areas). Although forecasted declines in mean overwintering population size appear relatively modest, at least in the near term (Figure 5a–c), there are notable risks to long-term viability as monarch population size can vary greatly from 1 year to the next. Given that the area occupied by overwintering monarchs is already perilously low, poor weather conditions (e.g., GDD well above 2004–2018 means) on the spring and summer breeding grounds in 1 year could drive the subsequent overwintering population size low enough that recruitment is unable to compensate for previous losses. Such a scenario, however, assumes that monarchs will not be able to adapt to changing conditions or expand their breeding ranges, as some invertebrate species have already done (e.g., Platts et al., 2019; Wilson et al., 2021). Because minimum viable population size is currently unknown, we used population forecasts to assess the likelihood that future overwintering populations would occupy less than 0.67 ha, the minimum value ever observed, which may overestimate extirpation risk.

While we used forecasts of overwintering population size to evaluate long-term monarch trends, forecasted population indices on the summer breeding grounds may be especially valuable for informing conservation efforts. Forecasted counts of adult monarchs throughout the Midwestern breeding grounds enable assessments of spatiotemporal variation in monarch abundance under a range of future scenarios. Although we are unable to account for potential northward expansion of the summer breeding range, our results suggest that there may be geographic shifts in local monarch abundance within the current range, driven by changes in both temperature (GDD) and precipitation. In particular, our analysis identified areas of the current summer breeding range where temperatures are likely to remain near 2004–2018 averages and precipitation is likely to increase, resulting in stable or even increasing monarch abundance (e.g., northern Ohio; Figure 4). Population declines are expected to be especially severe in northern parts of the breeding range, where GDD values are projected to greatly exceed values observed in the recent past. Such insights can be used to inform conservation strategies for monarchs and ensure that limited resources are allocated efficiently. Efforts to restore native grasslands and supplement milkweed populations, for example, may be most effective in locations where climate will be comparatively favorable for monarchs over the long term.

Our findings demonstrate the importance of considering ecological drivers across the full-annual cycle of a migratory species. For example, if our population forecasts had only accounted for projected changes in spring climate and assumed that summer climate

would be similar to that observed in the recent past, we would have underestimated potential declines in mean overwintering monarch population size by as much as 6%. Perhaps more importantly, failing to account for changes in temperature and precipitation on the summer breeding grounds would have prevented assessments of how the distribution of monarchs across the summer breeding grounds may shift in response to regional climate variation. For migratory species, limiting the scope of forecasts to only account for environmental changes that occur in a single season, or a subset of the migratory cycle, could lead to inefficient allocation of limited conservation resources (e.g., restoring habitat for monarchs where future climate is unlikely to be suitable) or at worst, flawed assessments of extirpation risk (Marra et al., 2015).

Although it may appear straightforward, decisions about which data should be used to characterize population responses to climate are challenging and will depend on the quality, spatial extent, and temporal scope of each data source. Longer time series may reduce parameter uncertainty, but only if it is safe to assume that the effects of climate or other factors in the model have remained constant over time (Rollinson et al., 2021). We used an expansive set of data from structured surveys over a recent 15-year period to characterize how the eastern monarch population responds to variation in climate and other environmental factors. Although we opted not to include a smaller set of data collected prior to 2004—as this imposed limitations on model structure and disregarded likely shifts in monarch population dynamics driven by changing management practices (Bahlai & Zipkin, 2020; Zylstra et al., 2021)—we explored how estimates of covariate effects might change with a longer time series of data by including additional, more limited, retrospective data on the monarch population (i.e., we evaluated a slightly modified model that included available data from 1999 to 2018; Table S3). Almost all parameter estimates, including effects of summer temperature and precipitation, were remarkably robust to the inclusion of 5 years of additional data (Table S3), corroborating patterns in forecasted abundance indices across the summer breeding range (Figure S5). However, the magnitude of spring temperature effects was smaller when additional data were included in the retrospective model, resulting in less severe projections of population declines with increases in spring temperatures (Figure S6). These results highlight the importance of carefully considering which datasets to incorporate in population forecasts and, critically, the value in assessing the impacts of these choices on the interpretation and use of predictions. For eastern monarchs, spatial patterns of forecasted abundance across the midwestern breeding grounds were relatively consistent with changes in the length of the retrospective dataset, suggesting that these forecasts can be reliably used for conservation even if there is uncertainty about the absolute magnitude of declines in overwintering monarch population size under future climate conditions.

The precision of population forecasts reflects our knowledge about future environmental changes and population responses to environmental variation (Dietze, 2017; Zylstra & Zipkin, 2021). Our analysis of uncertainties suggests that we can best improve precision of near-term monarch forecasts by collecting targeted data to more accurately and precisely estimate the relationships between breeding-season climate variables and monarch abundance, thereby reducing parameter uncertainty. In particular, using newly available data from volunteer-based networks to better understand lesser-studied portions of the migratory cycle (e.g., relationships between local climate conditions and spatiotemporal variation in abundance of monarchs in eastern Texas) would be especially valuable and is likely to improve the accuracy of population forecasts. Instigating studies in regions where climate is highly variable and/or changing rapidly (e.g., central Michigan; Figures 2 and 3; Crimmins & Crimmins, 2019; IPCC, 2014) would also be beneficial, as forecasts are less likely to be reliable when projected climate differs markedly from that used to estimate population responses to climatic change (Fitzpatrick & Hargrove, 2009; Saunders et al., 2016). Finally, recent efforts to systematically monitor monarchs and milkweed throughout the summer breeding range, like the Integrated Monarch Monitoring Program (Cariveau et al., 2019; Weiser et al., 2019), could improve precision of population forecasts by providing high-quality data on monarch recruitment in previously unsampled areas.

Migratory species play unique and critical roles in the functioning of ecosystems across the globe (Kirby et al., 2008; López-Hoffman et al., 2013). However, until recently, the scale and extent of long-distance migrations in the insect world, and the impacts of these mass migrations, have been largely unappreciated (Satterfield et al., 2020). The loss of migratory insects, like monarchs, is likely to have devastating ecological, economic, and cultural consequences. Conservation of these species is critical but challenging, given the geographic scope and wide range of potential threats. Reliable population forecasts that account for environmental changes both within and among seasonal ranges are needed to ensure the persistence of these iconic and charismatic species.

AUTHOR CONTRIBUTIONS

Erin R. Zylstra and Elise F. Zipkin contributed to conception of the research. Naresh Neupane contributed data. Erin R. Zylstra and Elise F. Zipkin constructed the model. Erin R. Zylstra ran analyses, and Erin R. Zylstra and Elise F. Zipkin wrote the first drafts of the paper. All authors contributed to the interpretation of results and edits to the paper.

ACKNOWLEDGMENTS

We thank the many public scientists that contributed to data collection. We also thank L. Ries for providing data and insights on monarch ecology and S. Saunders for providing comments on the manuscript. This work was supported by NSF grants: EF-1702635 (EFZ) and DBI-1954406 (EFZ) and by Grant No. G21AC10369-00 from the United States Geological Survey (USGS). Its contents are solely the responsibility of the authors and do not necessarily represent the views of the Midwest Climate Adaptation Science Center or the USGS. This manuscript is submitted for publication with the understanding that the United States Government is

authorized to reproduce and distribute reprints for Governmental purposes.

CONFLICT OF INTEREST

The authors declare no conflicts of interest.

DATA AVAILABILITY STATEMENT

Monarch data from the overwintering grounds, covariate data for 2004–2018, and climate projections are available on Zenodo (https://doi.org/10.5281/zenodo.5597600). Monarch data from the summer breeding grounds are proprietary and were obtained from the North American Butterfly Association (https://www.naba.org/), the Iowa Butterfly Survey Network (https://www.reimangardens.com/collections/insects/iowa-butterfly-survey-network/), the Illinois Butterfly Monitoring Network (https://ibmn.org/), the Michigan Butterfly Network (http://naturecenter.org/michiganbutterfly/), and the Ohio Lepidopterists (http://www.ohiolepidopterists.org/). These data may be available upon reasonable request from the aforementioned programs. Code needed to run analyses (R script, Stan model file) is available on Zenodo (https://doi.org/10.5281/zenodo.5597600).

ORCID

Erin R. Zylstra https://orcid.org/0000-0002-2536-0403
Naresh Neupane https://orcid.org/0000-0001-5652-0230
Elise F. Zipkin https://orcid.org/0000-0003-4155-6139

REFERENCES

Agrawal, A. A., & Inamine, H. (2018). Mechanisms behind the monarch's decline. *Science*, *360*, 1294–1296.
Bahlai, C. A., & Zipkin, E. F. (2020). The dynamic shift detector: An algorithm to identify changes in parameter values governing populations. *PLoS Computational Biology*, *16*, e1007542.
Both, C., Bouwhuis, S., Lessells, C. M., & Visser, M. E. (2006). Climate change and population declines in a long-distance migratory bird. *Nature*, *441*, 81–83.
Brower, L. P., Taylor, O. R., Williams, E. H., Slayback, D. A., Zubieta, R. R., & Ramírez, M. I. (2012). Decline of monarch butterflies overwintering in Mexico: Is the migratory phenomenon at risk? *Insect Conservation and Diversity*, *5*, 95–100.
Cariveau, A. B., Holt, H. L., Ward, J. P., Lukens, L., Kasten, K., Thieme, J., Caldwell, W., Tuerk, K., Baum, K. A., Drobney, P., Drum, R. G., Grundel, R., Hamilton, K., Hoang, C., Kinkead, K., McIntyre, J., Thogmartin, W. E., Turner, T., Weiser, E. L., … Oberhauser, K. (2019). The integrated monarch monitoring program: From design to implementation. *Frontiers in Ecology and Evolution*, *7*, 167.
Carpenter, B., Gelman, A., Hoffman, M. D., Lee, D., Goodrich, B., Betancourt, M., Brubaker, M., Guo, J., Li, P., & Riddell, A. (2017). Stan: A probabilistic programming language. *Journal of Statistical Software*, *76*, 1–32.
Cavanagh, R. D., Murphy, E. J., Bracegirdle, T. J., Turner, J., Knowland, C. A., Corney, S. P., Smith, W. O., Jr., Waluda, C. M., Johnston, N. M., Bellerby, R. G. J., Constable, A. J., Costa, D. P., Hofmann, E. E., Jackson, J. A., Staniland, I. J., Wolf-Gladrow, D., & Xavier, J. C. (2017). A synergistic approach for evaluating climate model output for ecological applications. *Frontiers in Marine Science*, *4*, 308.
Cayton, H. L., Haddad, N. M., Gross, K., Diamond, S. E., & Ries, L. (2015). Do growing degree days predict phenology across butterfly species? *Ecology*, *96*, 1473–1479.
Chen, I. C., Hill, J. K., Ohlemüller, R., Roy, D. B., & Thomas, C. D. (2011). Rapid range shifts of species associated with high levels of climate warming. *Science*, *333*, 1024–1026.
Couture, J. J., Serbin, S. P., & Townsend, P. A. (2015). Elevated temperature and periodic water stress alter growth and quality of common milkweed (*Asclepias syriaca*) and monarch (*Danaus plexippus*) larval performance. *Arthropod-Plant Interactions*, *9*, 149–161.
Crewe, T. L., Mitchell, G. W., & Larrivée, M. (2019). Size of the Canadian breeding population of monarch butterflies is driven by factors acting during spring migration and recolonization. *Frontiers in Ecology and Evolution*, *7*, 308.
Crimmins, T. M., & Crimmins, M. A. (2019). Biologically-relevant trends in springtime temperatures across the United States. *Geophysical Research Letters*, *46*, 12377–12387.
Culbertson, K. A., Garland, M. S., Walton, R. K., Zemaitis, L., & Pocius, V. M. (2022). Long-term monitoring indicates shifting fall migration timing in monarch butterflies (*Danaus plexippus*). *Global Change Biology*, *28*, 727–738.
Curley, S. R., Manne, L. L., & Veit, R. R. (2020). Differential winter and breeding range shifts: Implications for avian migration distances. *Diversity and Distributions*, *26*, 415–425.
Dietze, M. C. (2017). *Ecological forecasting*. Princeton University Press.
Diffenbaugh, N. S., & Field, C. B. (2013). Changes in ecologically critical terrestrial climate conditions. *Science*, *341*, 486–492.
Doyle, S., Cabot, D., Walsh, A., Inger, R., Bearhop, S., & McMahon, B. J. (2020). Temperature and precipitation at migratory grounds influence demographic trends of an Arctic-breeding bird. *Global Change Biology*, *26*, 5447–5458.
Edwards, C. B., & Crone, E. E. (2021). Estimating abundance and phenology from transect count data with GLMs. *Oikos*, *130*, 1335–1345.
Eyring, V., Bony, S., Meehl, G. A., Senior, C. A., Stevens, B., Stouffer, R. J., & Taylor, K. E. (2016). Overview of the coupled model Intercomparison project phase 6 (CMIP6) experimental design and organization. *Geoscientific Model Development*, *9*, 1937–1958.
Fitzpatrick, M. C., & Hargrove, W. W. (2009). The projection of species distribution models and the problem of non-analog climate. *Biodiversity and Conservation*, *18*, 2255–2261.
Flockhart, D. T. T., Brower, L. P., Ramírez, M. I., Hobson, K. A., Wassenaar, L. I., Altizer, S., & Norris, E. R. (2017). Regional climate on the breeding grounds predicts variation in the natal origin of monarch butterflies overwintering in Mexico over 38 years. *Global Change Biology*, *23*, 2565–2576.
Gauthier, G., Péron, G., Lebreton, J. -D., Grenier, P., & van Oudenhove, L. (2016). Partitioning prediction uncertainty in climate-dependent population models. *Proceedings of the Royal Society B: Biological Sciences*, *283*, 20162353.
Gelman, A., & Rubin, D. B. (1992). Inference from iterative simulation using multiple sequences. *Statistical Science*, *7*, 457–472.
Green, K., Caley, P., Baker, M., Dreyer, D., Wallace, J., & Warrant, E. (2021). Australian Bogong moths *Agrotis infusa* (lepidoptera: Noctuidae), 1951–2020: Decline and crash. *Austral Entomology*, *60*, 66–81.
Haan, N. L., & Landis, D. A. (2020). Grassland disturbance effects on first-instar monarch butterfly survival, floral resources, and flower-visiting insects. *Biological Conservation*, *243*, 108492.
Halsch, C. A., Shapiro, A. M., Fordyce, J. A., Nice, C. C., Thorne, J. H., Waetjen, D. P., & Forister, M. L. (2021). Insects and recent climate change. *Proceedings of the National Academy of Sciences of the United States of America*, *118*, e2002543117.
Harris, R. M. B., Grose, M. R., Lee, G., Bindoff, N. L., Porfirio, L. L., & Fox-Hughes, P. (2014). Climate projections for ecologists. *WIREs Climate Change*, *5*, 621–637.
Hawkins, E., & Sutton, R. (2009). The potential to narrow uncertainty in regional climate predictions. *Bulletin of the American Meteorological Society*, *90*, 1095–1107.
Huey, R. B., Kearney, M. R., Krockenberger, A., Holtum, J. A. M., Jess, M., & Williams, S. E. (2012). Predicting organismal vulnerability to

climate warming: Roles of behaviour, physiology and adaptation. *Philosophical Transactions of the Royal Society B: Biological Sciences*, *367*, 1665–1679.

Iles, D., & Jenouvrier, S. (2019). Projected population consequences of climate change. In P. O. Dunn & A. P. Møller (Eds.), *Effects of climate change on birds* (pp. 147–164). Oxford University Press.

IPCC. (2014). *Climate change 2014: Impacts, adaptation, and vulnerability*. Cambridge University Press.

Jenouvrier, S., Holland, M., Iles, D., Labrousse, S., Landrum, L., Garnier, J., Caswell, H., Weimerskirch, H., LaRue, M., Ji, R., & Barbraud, C. (2020). The Paris agreement objections will likely halt future declines of emperor penguins. *Global Change Biology*, *26*, 1170–1184.

Jenouvrier, S., Holland, M., Stroeve, J., Barbraud, C., Weimerskirch, H., Serreze, M., & Caswell, H. (2012). Effects of climate change on an emperor penguin population: Analysis of coupled demographic and climate models. *Global Change Biology*, *18*, 2756–2770.

Jenouvrier, S., Judy, C.-C., Wolf, S., Holland, M., Labrousse, S., LaRue, M., Wienecke, B., Fretwell, P., Barbraud, C., Greenwald, N., Stroeve, J., & Trathan, P. N. (2021). The call of the emperor penguin: Legal responses to species threatened by climate change. *Global Change Biology*, *27*, 5008–5029.

Karmalkar, A. V., Thibeault, J. M., Bryan, A. M., & Seth, A. (2019). Identify credible and diverse GCMs for regional climate change studies–case study: Northeastern United States. *Climatic Change*, *154*, 367–386.

Kirby, J. S., Stattersfield, A. J., Butchart, S. H. M., Evans, M. I., Grimmett, R. F. A., Jones, V. R., O'Sullivan, J., Tucker, G. M., & Newton, I. (2008). Key conservation issues for migratory land- and waterbird species on the world's major flyways. *Bird Conservation International*, *18*, S49–S73.

Layton-Matthews, K., Hansen, B. B., Grøtan, V., Fuglei, E., & Loonen, M. J. J. E. (2020). Contrasting consequences of climate change for migratory geese: Predation, density dependence and carryover effects offset benefits of high-arctic warming. *Global Change Biology*, *26*, 642–657.

Lemoine, N. P. (2015). Climate change may alter breeding ground distributions of eastern migratory monarchs (*Danaus plexippus*) via range expansion of Asclepias host plants. *PLoS ONE*, *10*, e0118614.

López-Hoffman, L., Semmens, D. J., & Diffendorfer, J. E. (2013). How do migratory species add ecosystem service value to wilderness? Calculating the spatial subsidies provided by protected areas. *International Journal of Wilderness*, *19*, 14–19.

Marra, P. P., Cohen, E. B., Loss, S. R., Rutter, J. E., & Tonra, C. M. (2015). A call for full annual cycle research in animal ecology. *Biology Letters*, *11*, 20150552.

Neupane, N., Zipkin, E. F., Saunders, S. P., & Ries, L. (2022). Grappling with uncertainty in ecological projections: A case study using the migratory monarch butterfly. *Ecosphere*, *13*, e03874.

Oberhauser, K. S., Ries, L., Altizer, S., Batalden, R. V., Kudell-Ekstrum, J., Garland, M., Howard, E., Jepsen, S., Lovett, J., Monroe, M., Morris, G., Rendón-Salinas, E., RuBino, R. G., Ryan, A., Taylor, O. R., Treviño, R., Villablanca, F. X., & Walton, D. (2015). Contributions to monarch biology and conservation through citizen science. In K. S. Oberhauser, K. S. Nail, & S. Altizer (Eds.), *Monarchs in a changing world: Biology and conservation of an iconic butterfly* (pp. 13–30). Cornell University Press.

O'Neill, B. C., Kriegler, E., Ebi, K. L., Kemp-Benedict, E., Riahi, K., Rothman, D. S., van Ruijven, B. J., van Vuuren, D. P., Birkmann, J., Kok, K., Levy, M., & Solecki, W. (2017). The roads ahead: Narratives for shared socioeconomic pathways describing world futures in the 21st century. *Global Environmental Change*, *42*, 169–180.

O'Neill, B. C., Tebaldi, C., van Vuuren, D. P., Eyring, V., Friedlingstein, P., Hurtt, G., Knutti, R., Kriegler, E., Lamarque, J.-F., Lowe, J., Meehl, G. A., Moss, R., Riahi, K., & Sanderson, B. M. (2016). The scenario model Intercomparison project (ScenarioMIP) for CMIP6. *Geoscientific Model Development*, *9*, 3461–3482.

Parmesan, C. (2006). Ecological and evolutionary responses to recent climate change. *Annual Review of Ecology, Evolution, and Systematics*, *37*, 637–669.

Platts, P. J., Mason, S. C., Palmer, G., Hill, J. K., Oliver, T. H., Powney, G. D., Fox, R., & Thomas, C. D. (2019). Habitat availability explains variation in climate-driven range shifts across multiple taxonomic groups. *Scientific Reports*, *9*, 15039.

Pomara, L. Y., LeDee, O. E., Martin, K. J., & Zuckerberg, B. (2014). Demographic consequences of climate change and land cover help explain a history of extirpation and range contraction in a declining snake species. *Global Change Biology*, *20*, 2087–2099.

Post, E., & Forchhammer, M. C. (2008). Climate change reduced reproductive success of an Arctic herbivore through trophic mismatch. *Philosophical Transactions of the Royal Society B: Biological Sciences*, *363*, 2369–2375.

R Core Team. (2021). *R: A language and environment for statistical computing*. R Foundation for Statistical Computing. https://www.R-project.org/

Rabaiotti, D., & Woodroffe, R. (2019). Coping with climate change: Limited behavioral responses to hot weather in a tropical carnivore. *Oecologia*, *189*, 587–599.

Ramírez, M. I., Gímenez-Azcárate, J., & Luna, L. (2003). Effects of human activities on monarch butterfly habitat in protected mountain forests, Mexico. *Forestry Chronicle*, *79*, 242–246.

Ramírez, M. I., López-Sánchez, J. G., & Barrasa, S. (2019). *Mapa de Vegetación y Cubiertas del Suelo, Reserva de la Biosfera Mariposa Monarca*. Serie Cartográfica Monarca, Volumen II. CIGA-UNAM.

Ramírez, M. I., Miranda, R., Zubieta, R., & Jiménez, M. (2007). Land cover and road network map for the monarch butterfly biosphere Reserve in Mexico, 2003. *Journal of Maps*, *3*, 181–190.

Ramírez, M. I., Sáenz-Romero, C., Rehfeldt, G., & Salas-Canela, L. (2015). Threats to the availability of overwintering habitat in the monarch butterfly biosphere reserve: Land use and climate change. In K. S. Oberhauser, K. S. Nail, & S. Altizer (Eds.), *Monarchs in a changing world: Biology and conservation of an iconic butterfly* (pp. 157–168). Cornell University Press.

Ries, L., Taron, D. J., Rendón-Salinas, E., & Oberhauser, K. S. (2015). Connecting eastern monarch population dynamics across their migratory cycle. In K. S. Oberhauser, K. S. Nail, & S. Altizer (Eds.), *Monarchs in a changing world: Biology and conservation of an iconic butterfly* (pp. 268–282). Cornell University Press.

Rollinson, C. R., Finley, A. O., Alexander, M. R., Banerjee, S., Hamil, K. D., Koenig, L. E., Locke, D. H., DeMarche, M. L., Tingley, M. W., Wheeler, K., Youngflesh, C., & Zipkin, E. F. (2021). Working across space and time: Nonstationarity in ecological research and application. *Frontiers in Ecology and the Environment*, *19*, 66–72.

Rosenberg, K. V., Dokter, A. M., Blancher, P. J., Sauer, J. R., Smith, A. C., Smith, P. A., Stanton, J. C., Panjabi, A., Helft, L., Parr, M., & Marra, P. P. (2019). Decline of the north American avifauna. *Science*, *366*, 120–124.

Roy, D. B., Rothery, P., Moss, D., Pollard, E., & Thomas, J. A. (2001). Butterfly numbers and weather: Predicting historical trends in abundance and the future effects of climate change. *Journal of Animal Ecology*, *70*, 201–217.

Satterfield, D. A., Sillett, T. S., Chapman, J. W., Altizer, S., & Marra, P. P. (2020). Seasonal insect migrations: Massive, influential, and overlooked. *Frontiers in Ecology and the Environment*, *18*, 335–344.

Saunders, S. P., Ries, L., Neupane, N., Ramírez, M. I., García-Serrano, E., Rendón-Salinas, E., & Zipkin, E. F. (2019). Multiscale seasonal factors drive the size of winter monarch colonies. *Proceedings of the National Academy of Sciences of the United States of America*, *116*, 8609–8614.

Saunders, S. P., Ries, L., Oberhauser, K. S., Thogmartin, W. E., & Zipkin, E. F. (2018). Local and cross-seasonal associations of climate and land use with abundance of monarch butterflies. *Ecography*, *41*, 278–290.

Saunders, S. P., Ries, L., Oberhauser, K. S., & Zipkin, E. F. (2016). Evaluating confidence in climate-based predictions of population change in a migratory species. *Global Ecology and Biogeography*, *25*, 1000–1012.

Schultz, C. B., Brown, L. M., Pelton, E., & Crone, E. E. (2017). Citizen science monitoring demonstrates dramatic declines of monarch butterflies in western North America. *Biological Conservation*, *214*, 343–346.

Senner, N. R., Stager, M., & Sandercock, B. K. (2017). Ecological mismatches are moderated by local conditions for two populations of a long-distance migratory bird. *Oikos*, *126*, 61–72.

Stan Development Team. (2018). *rstan: The R Interface to Stan*. R Package Version 2.17.3. http://mc-stan.org/

Thogmartin, W. E., Diffendorfer, J. E., López-Hoffman, L., Oberhauser, K., Pleasants, J., Semmens, B. X., Semmens, D., Taylor, O. R., & Wiederholt, R. (2017). Density estimates of monarch butterflies overwintering in Central Mexico. *PeerJ*, *5*, e3221.

Thornton, P. E., Thornton, M. M., Mayer, B. W., Wei, Y., Devarakonda, R., Vose, R. S., & Cook, R. B. (2018). *Daymet: Daily Surface Weather Data on a 1-km Grid for North America, Version 3*. ORNL DAAC. https://doi.org/10.3334/ORNLDAAC/1328

U.S. Fish and Wildlife Service. (2020). Endangered and threatened wildlife and plants; 12-month finding for the monarch butterfly. *Federal Register*, *85*, 81813–81822.

Vidal, O., & Rendón-Salinas, E. (2014). Dynamics and trends of overwintering colonies of the monarch butterfly in Mexico. *Biological Conservation*, *180*, 165–175.

Weiser, E. L., Diffendorfer, J. E., Grundel, R., López-Hoffman, L., Pecoraro, S., Semmens, D., & Thogmartin, W. E. (2019). Balancing sampling intensity against spatial coverage for a community science monitoring programme. *Journal of Applied Ecology*, *56*, 2252–2263.

Wilson, J. K., Casajus, N., Hutchinson, R. A., McFarland, K. P., Kerr, J. T., Berteaux, D., Larrivée, M., & Prudic, K. L. (2021). Climate change and local host availability drive the northern range boundary in the rapid expansion of a specialist insect herbivore, *Papilio cresphontes*. *Frontiers in Ecology and Evolution*, *9*, 579230.

Zalucki, M. P. (1982). Temperature and rate of development in *Danaus plexippus* L. and *D. chrysippus* L. (lepidoptera: Nymphalidae). *Austral Journal of Entomology*, *21*, 241–246.

Zipkin, E. F., Ries, L., Reeves, R., Regetz, J., & Oberhauser, K. S. (2012). Tracking climate impacts on the migratory monarch butterfly. *Global Change Biology*, *18*, 3039–3049.

Zurell, D., Graham, C. H., Gallien, L., Thuiller, W., & Zimmermann, N. E. (2018). Long-distance migratory birds threatened by multiple independent risks from global change. *Nature Climate Change*, *8*, 992–996.

Zylstra, E. R., Neupane, N., & Zipkin, E. F. (2022). Code and data for "multi-season climate projections forecast declines in migratory monarch butterflies". *Zenodo*, https://doi.org/10.5281/zenodo.5597600

Zylstra, E. R., Ries, L., Neupane, N., Saunders, S. P., Ramírez, M. I., Rendón-Salinas, E., Oberhauser, K. S., Farr, M. T., & Zipkin, E. F. (2021). Changes in climate drive recent monarch butterfly dynamics. *Nature Ecology and Evolution*, *5*, 1441–1452.

Zylstra, E. R., & Zipkin, E. F. (2021). Accounting for sources of uncertainty when forecasting population responses to climate change. *Journal of Animal Ecology*, *90*, 558–561.

SUPPORTING INFORMATION

Additional supporting information can be found online in the Supporting Information section at the end of this article.

How to cite this article: Zylstra, E. R., Neupane, N., & Zipkin, E. F. (2022). Multi-season climate projections forecast declines in migratory monarch butterflies. *Global Change Biology*, *28*, 6135–6151. https://doi.org/10.1111/gcb.16349